

Personalized Mood Prediction from Patterns of Behavior Collected with Smartphones

Supplemental Material

Brunilda Balliu*^{1,2,3}, Chris Douglas⁴, Darsol Seok⁵, Liat Shenhav⁶, Yue Wu⁶, Doxa Chatzopoulou⁵, William Kaiser⁷, Victor Chen⁷, Jennifer Kim⁵, Sandeep Deverasetty⁵, Inna Arnaudova⁵, Robert Gibbons⁸, Eliza Congdon^{4,5}, Michelle G. Craske^{4,9}, Nelson Freimer^{4,10}, Eran Halperin⁶, Sriram Sankararaman^{1,6,10}, Jonathan Flint^{4,10*}

¹Departments of Computational Medicine, University of California Los Angeles, Los Angeles, USA,

²Departments of Pathology and Laboratory Medicine, University of California Los Angeles, Los Angeles, USA,

³Department of Biostatistics, University of California Los Angeles, Los Angeles, USA,

⁴Department of Psychiatry and Biobehavioral Science, University of California Los Angeles, Los Angeles, USA,

⁵Semel Institute for Neuroscience and Human Behavior, University of California Los Angeles, Los Angeles, USA,

⁶Department of Computer Science, University of California Los Angeles, Los Angeles, USA,

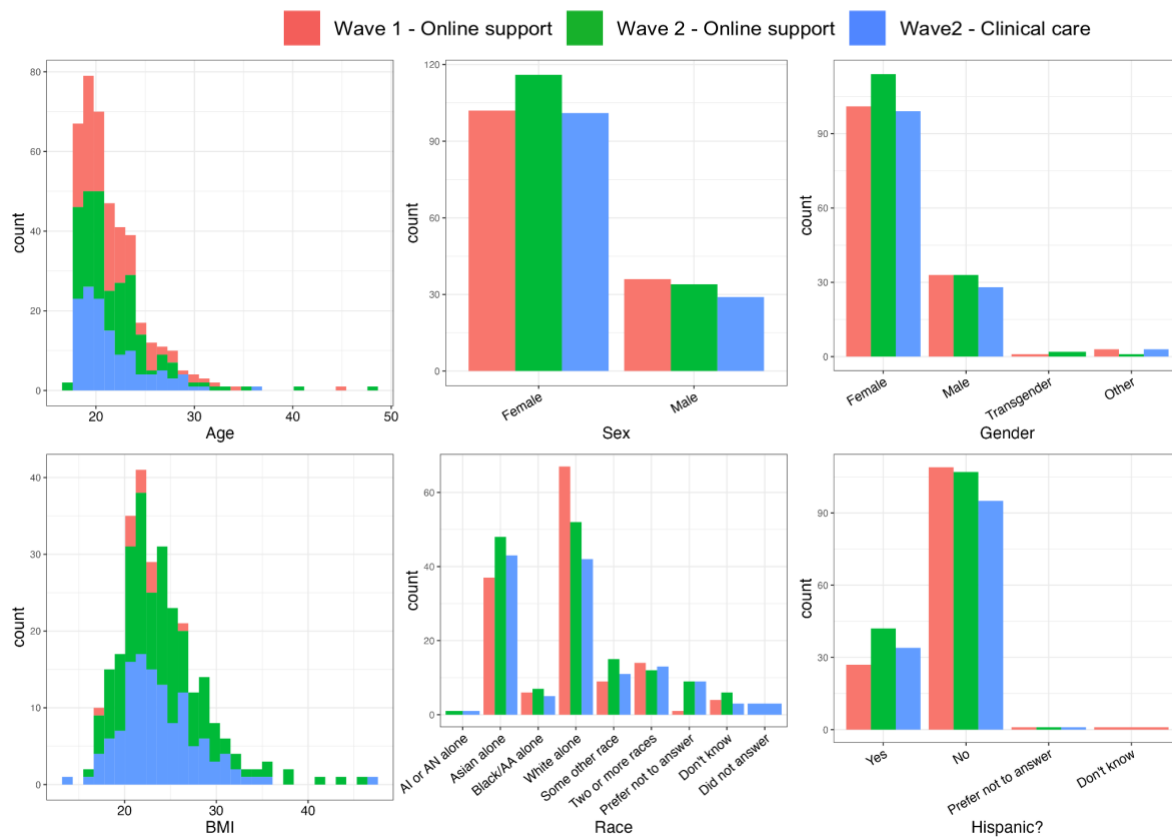
⁷Department of Electrical Engineering, University of California Los Angeles, Los Angeles, USA,

⁸Departments of Medicine, Public Health Sciences and Comparative Human Development, University of Chicago, USA

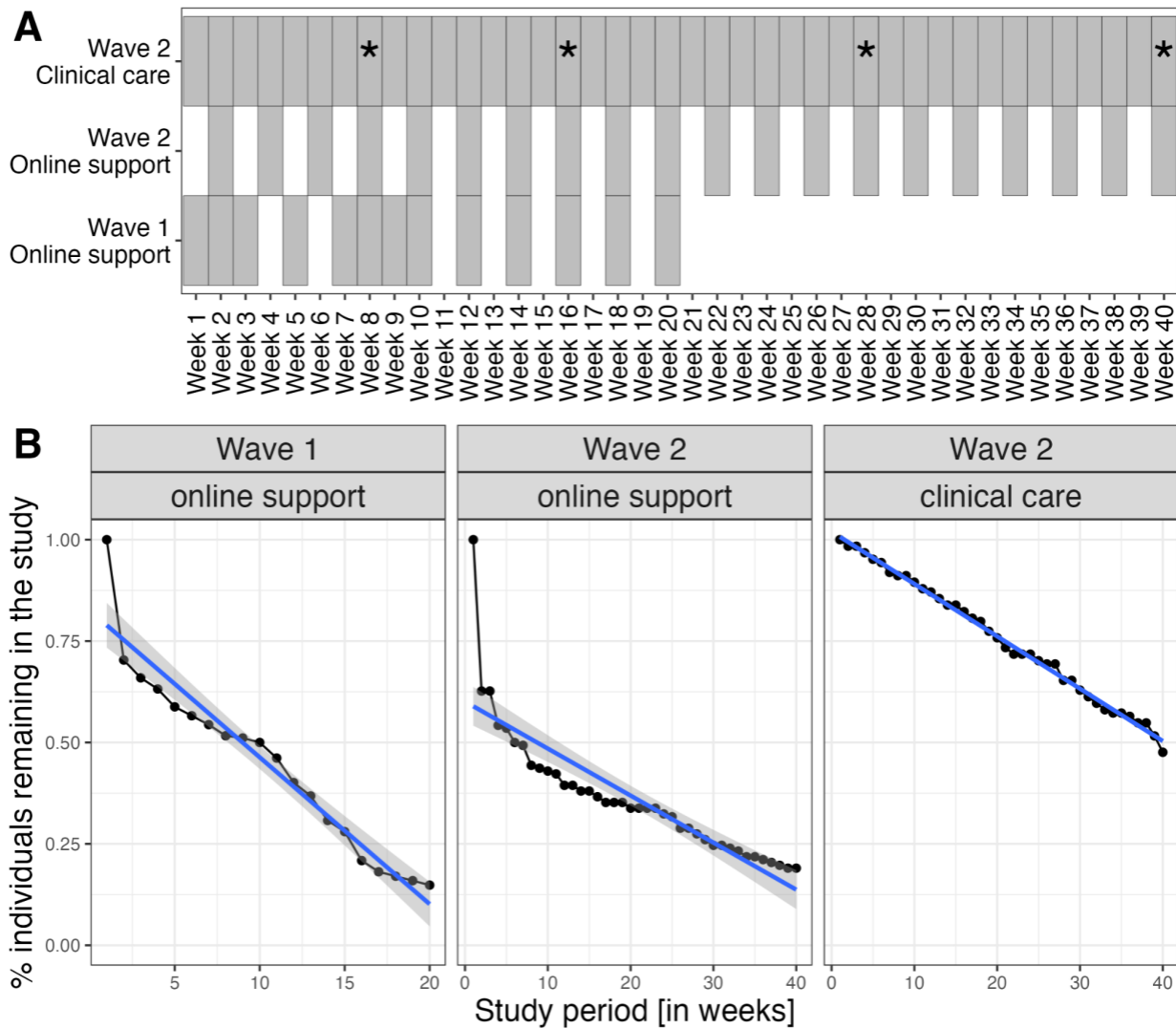
⁹Department of Psychology, University of California Los Angeles, Los Angeles, USA,

¹⁰Department of Human Genetics, University of California Los Angeles, Los Angeles, USA

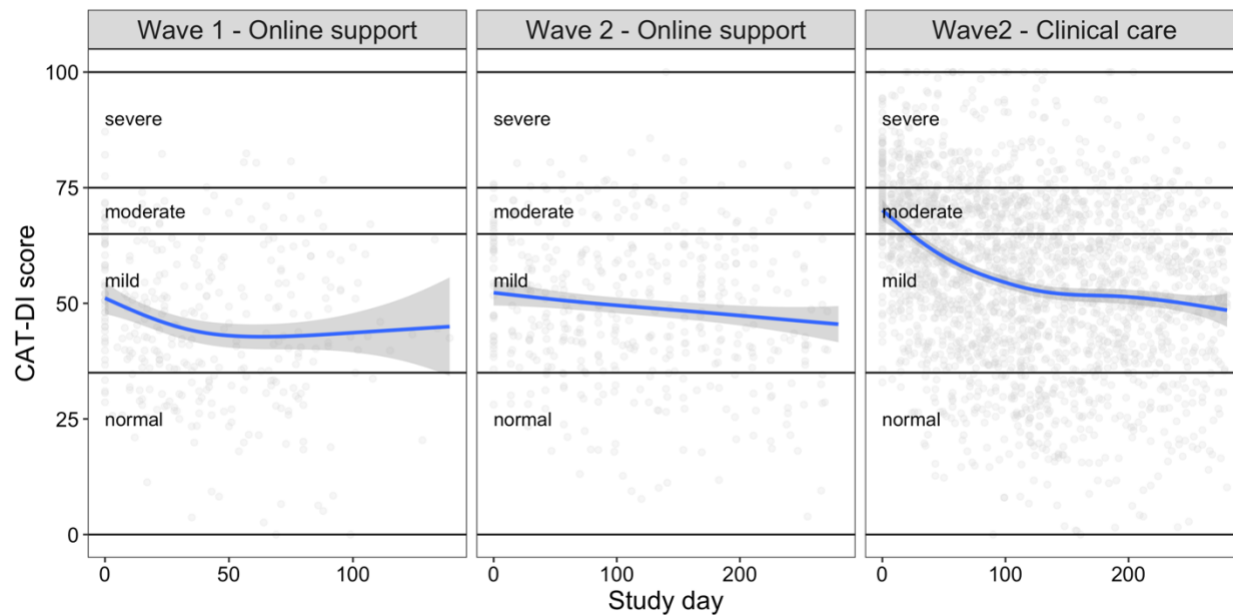
* Corresponding authors (emails: balliu@ucla.edu and Jflint@mednet.ucla.edu)



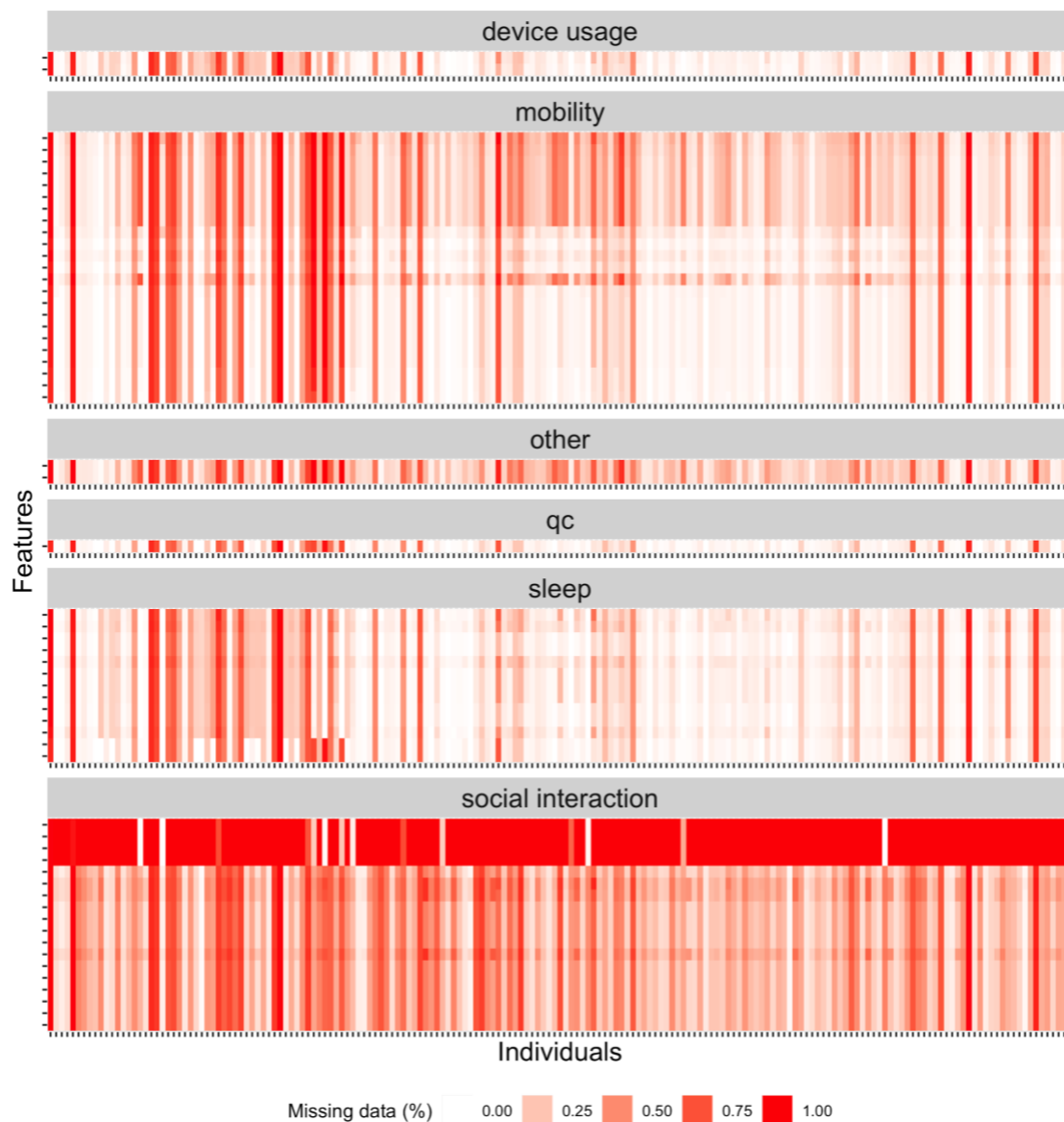
Supplementary Figure 1: **Demographic information for participants in each wave.** First row: histogram of age and bar plot of sex and gender. Second row: histogram of BMI and bar plot of race and ethnicity. Color indicates wave and treatment protocol combination. AI or AN: American Indian or Alaska Native. AA: African American.



Supplementary Figure 2: **CAT-DI administration protocol and compliance with CAT-DI assessment protocol for each wave and treatment group.** (A) CAT-DI administration schedule. Each box indicates a week during which participants in each group were expected to complete the CAT-DI. Asterisks indicate weeks with additional in-person administrations of CAT-DI for Wave 2 participants which received clinical care. (B) Participant CAT-DI retention rate for each enrollment wave and treatment group. The x-axis shows weeks from the beginning of the study for each participant while the y axis shows the proportion of individuals that were still completing the CAT-DI at that week. The continuous lines show the linear regression fit with 95% confidence intervals (gray shading).



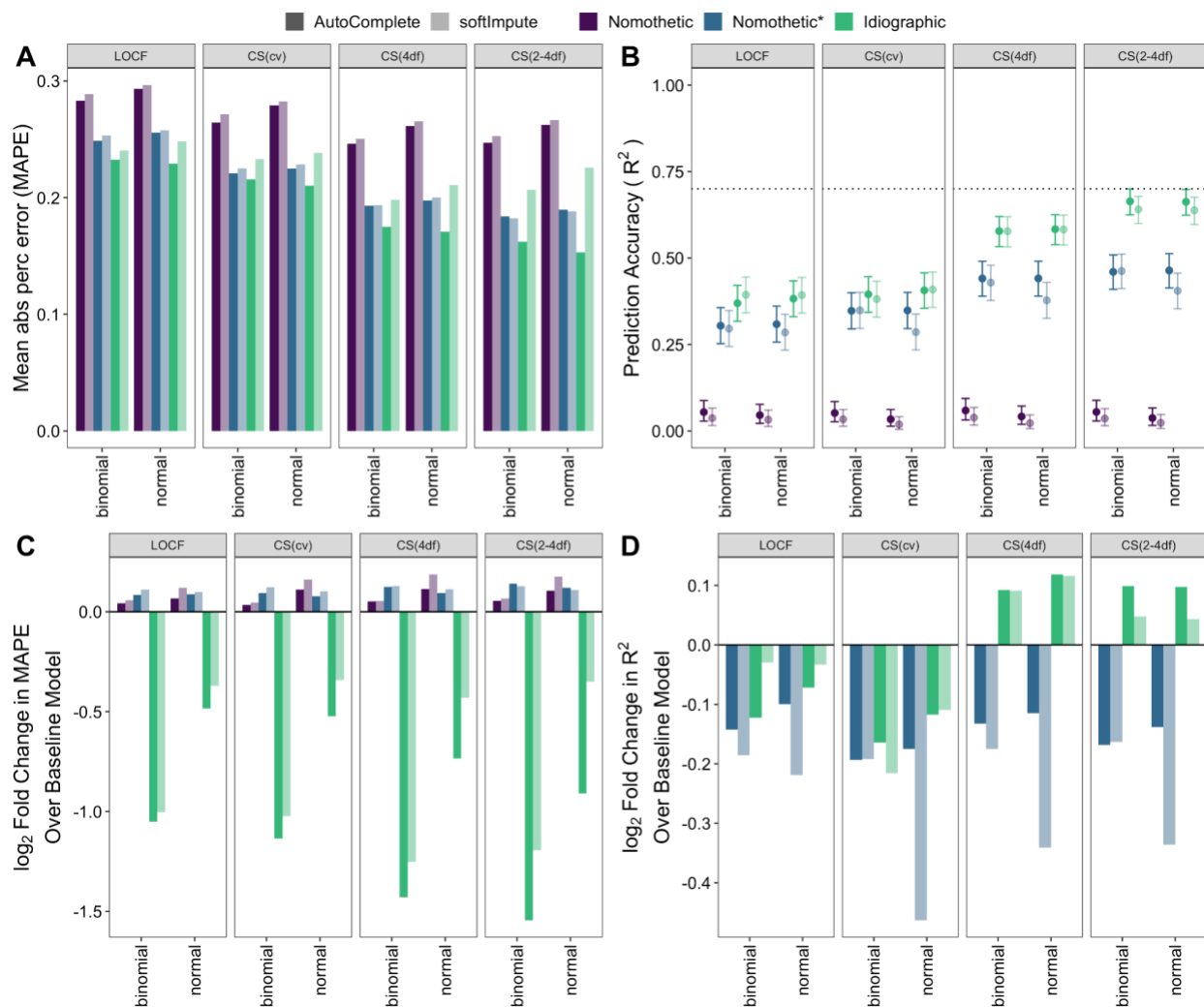
Supplementary Figure 3: **Effect of therapy per wave and treatment group.** The x-axis shows the study day with zero indicating the first day of CAT-DI assessment for each individual. The y-axis indicates the CAT-DI severity score for each individual / day in the study. The blue line indicates the fit of a generalized additive model with $y \sim s(\text{day} + \text{wave: treatment group}, \text{bs} = "cs")$ and gaussian family.



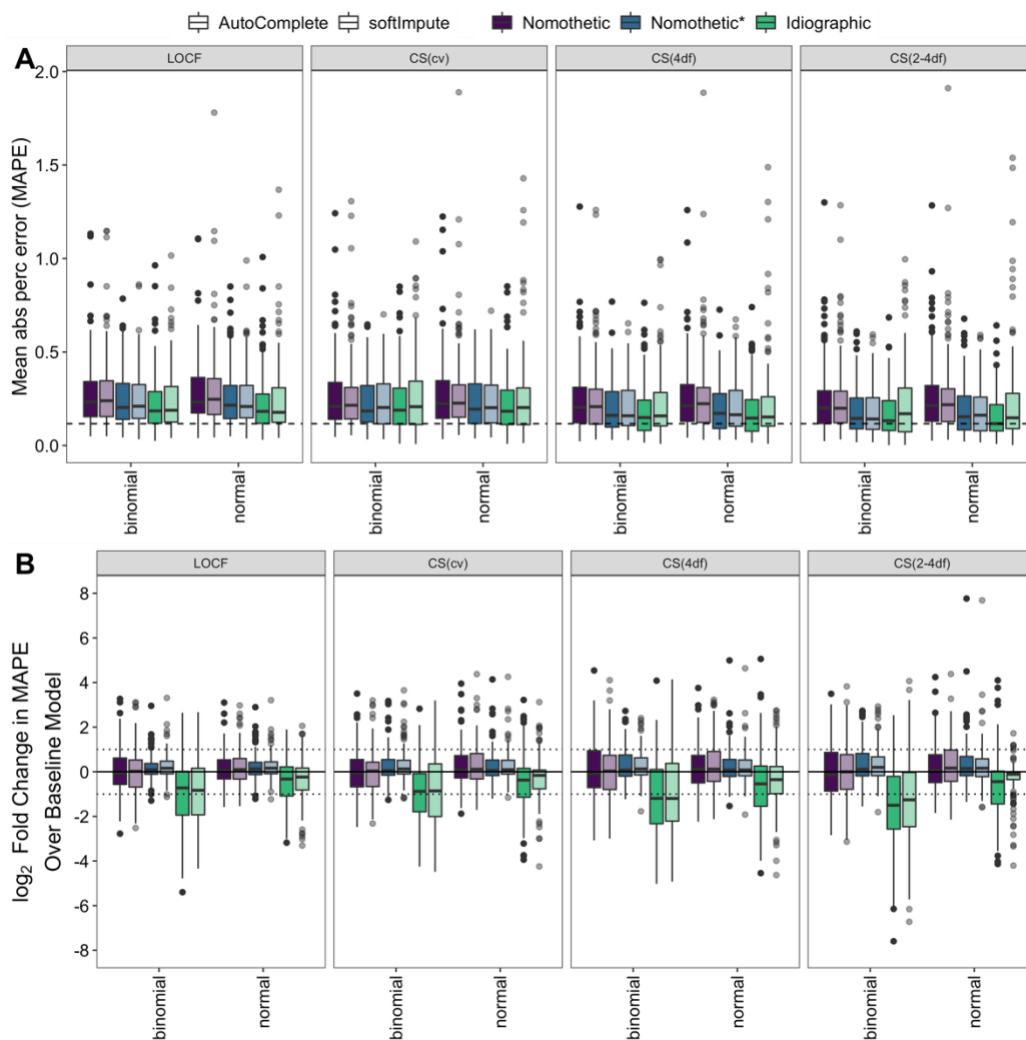
Supplementary Figure 4: **Missing feature data summary.** Heat map showing missing data percentage in each of the four types of features extracted from smartphone data for all individuals. Each tick on the x-axis (y-axis) represents an individual (feature). For ease of plotting, we have excluded transformation-based features. For participants with iOS devices (majority of individuals), we did not have any information on social interaction features related to text message information due to permission. These features are excluded from analyses when considering individuals with iOS devices.

		Depressed mood	Diminished interest or loss of pleasure activities (anhedonia)	Weight change or appetite disturbance	Sleep disturbance	Psychomotor agitation or retardation	Fatigue or loss of energy	Feelings of worthlessness	Diminished concentration; indecisiveness	Suicidal ideation/intent
Mobility features	Variance in latitude		•							
	Variance in longitude		•							
	Number of locations visited in total		•							
	Number of locations visited at night		•							
	Number of locations visited during the day		•							
	Number of locations visited in the evening		•							
	Location entropy over full day		•							
	Location entropy over full day (normalized)		•							
	Location entropy at night		•							
	Location entropy at night (normalized)		•							
	Location entropy during the day		•							
	Location entropy during the day (normalized)		•							
	Location entropy in the evening		•							
	Location entropy in the evening (normalized)		•							
	Time spent at home total (hours)		•				•			
	Time spent at home at night (hours)		•				•			
	Time spent at home during the day (hours)		•				•			
	Time spent at home in the evening (hours)		•				•			
	Percentage of time spent at home in total (%)		•				•			
	Percentage of time spent at home at night (%)		•				•			
Percentage of time spent at home during the day (%)		•				•				
Percentage of time spent at home in the evening (%)		•				•				
Phone interactions	Number of phone interactions during day							•		
	Number of phone interactions at night							•		
Sleep	Duration of longest phone off period (hours)				•					
	Beginning of longest phone off period				•					
	End of longest phone off period				•					
	Phone on duration midnight to 8am (hours)				•					
	Phone off duration midnight to 8am (hours)				•					
	Percentage of time phone on midnight to 8am (%)				•					
	Time of nadir of phone interactions				•					
Social interaction	Total number of calls		•							
	Number of incoming calls attempted		•							
	Number of outgoing calls attempted		•							
	Number of completed calls		•							
	Number of missed calls		•							
	Number of unanswered outgoing calls		•							
	Percentage of completed outgoing calls (%)		•							
	Percentage of unanswered outgoing calls (%)		•							
	Duration of incoming calls (minutes)		•							
	Duration of outgoing calls (minutes)		•							
	Total time spent on phone (minutes)		•							
	Average duration per call (minutes)		•							
	Duration of outgoing calls (%)		•							
	Number of distinct message contacts		•							
	Total number of messages		•							
	Number of incoming messages		•							
	Number of outgoing messages		•							
	Percent of messages outgoing		•							

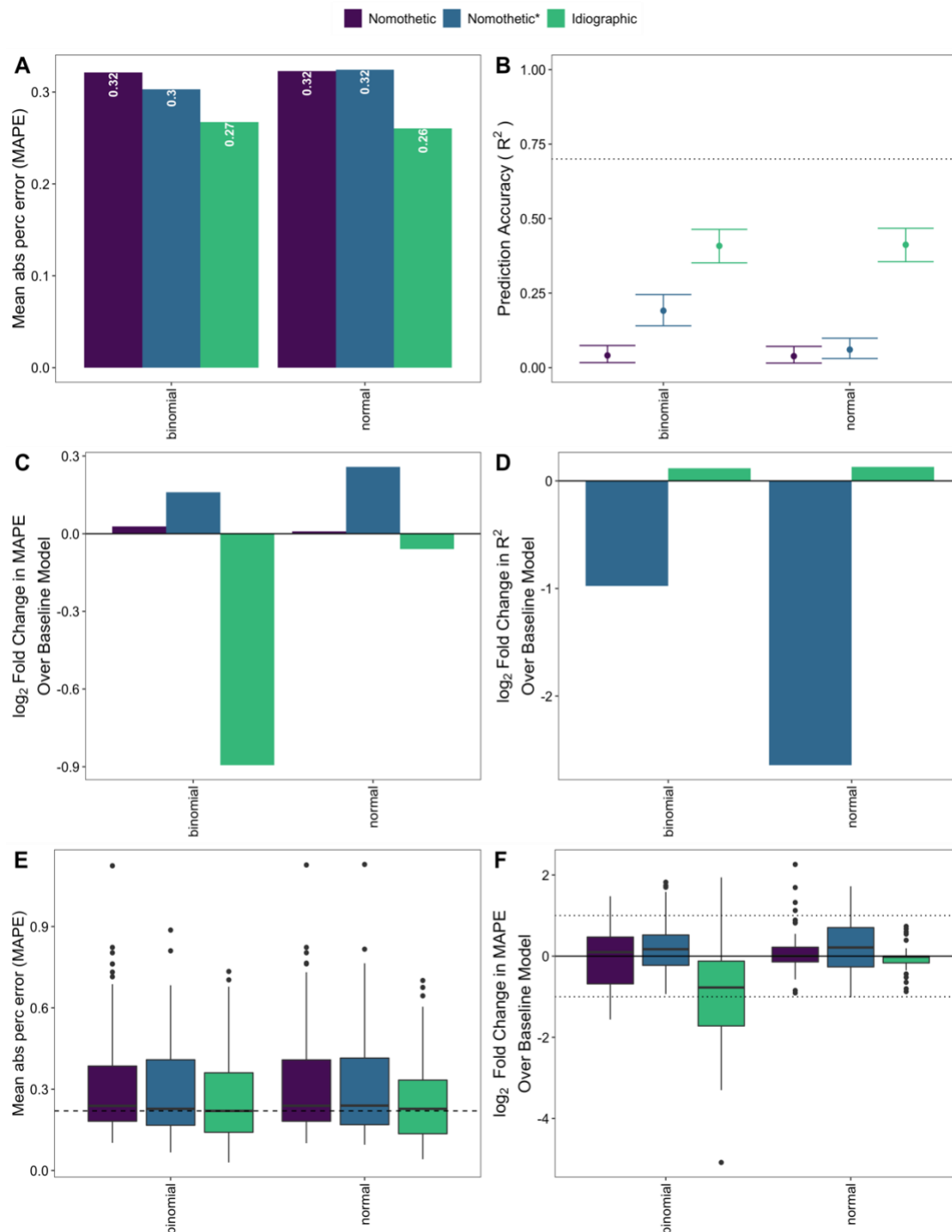
Supplementary Figure 5: **Mapping of sensor-derived behavioral features to DSM5 Major Depressive Disorder criteria.** The individual behavioral features derived from phone sensors map primarily to the DSM criteria of disrupted sleep, loss of energy, and anhedonia. Each of these base features is further transformed to look for deviations from individual baseline over varying time scales (e.g., last day's deviation from the weekly average) to arrive at the final set of behavioral features.



Supplementary Figure 6: **Idiographic models achieve higher group level prediction accuracy than nomothetic models.** (A-B) CAT-DI prediction accuracy across all individuals in the test set as measured by MAPE (A) and R^2 (B) across all individuals for different latent depression traits (panel), modeling approaches (color), CAT-DI regression model (x-axis), and feature imputation methods (transparency). The dotted line in B indicates 70% prediction accuracy and bars indicate 95% confidence intervals of R^2 . (C-D) \log_2 fold change in CAT-DI prediction accuracy, as measured by MAPE (C) and R^2 (D), of feature-based model over the baseline model for different latent depression traits, modeling approaches, CAT-DI regression models, and feature imputation methods. Negative \log_2 fold change in MAPE and positive \log_2 fold change in R^2 mean that the feature-based model performs better than the baseline model. A \log_2 fold change in MAPE of -1 means that the prediction error of the baseline model is twice as large as that of the feature based model. MAPE: mean absolute percent error. LOCF: last observation carried forward. CS(xdf): cubic spline with x degrees of freedom. CS(cv): best-fitting cubic spline according to leave-one-out cross-validation.



Supplementary Figure 7: **Idiographic models achieve higher individual-level prediction accuracy than nomothetic models.** Box plots of MAPE distribution of feature-based model (A) and log₂ fold change in CAT-DI prediction accuracy of feature-based model over the baseline model (B) across individuals for different latent depression traits (panel), modeling approaches (color), CAT-DI regression model (x-axis), and feature imputation methods (transparency). All plots are based on individuals with at least five assessments in the test set ($N=143$). The dark black line represents the median value; the box limits show the interquartile range (IQR) from the first (Q1) to third (Q3) quartiles; the whiskers extend to the furthest data point within $Q1-1.5*IQR$ (bottom) and $Q3+1.5*IQR$ (top). LOCF: last observation carried forward. CS(xdf): cubic spline with x degrees of freedom. CS(cv): best-fitting cubic spline according to leave-one-out cross-validation.



Supplementary Figure 8: Idiographic models achieve higher group and individual level prediction accuracy than nomothetic models when CAT-DI is modeled at the (bi)weekly level. (A-D) Population-level CAT-DI prediction accuracy of the feature-based model (A-B) and \log_2 fold change in population-level CAT-DI prediction accuracy of the feature-based model over the baseline model (C-D) as measured by MAPE (A and C) and R^2 (B and D) across all individuals in the test set for different modeling approaches (color) and CAT-DI regression model (x-axis). The dotted line in B indicates 70% prediction accuracy and the bars indicate 95% confidence intervals of R^2 . (E-F) Box plots of MAPE distribution of feature-based model (E) and \log_2 fold change in CAT-DI prediction accuracy of feature-based model over the baseline model (F) in the test set across individuals for different modeling approaches (color) and CAT-DI regression model (x-axis). The dark black line represents the median value; the box limits show the interquartile range (IQR) from the first (Q1) to third (Q3) quartiles; the whiskers extend to the furthest data point within $Q1-1.5*IQR$ (bottom) and $Q3+1.5*IQR$ (top). Plots E-F are based on individuals with at least five assessments in the test set ($N=143$). For all six plots, features were imputed using AutoComplete. MAPE: mean absolute percentage error.